ECG Fiducial Points Extraction Using Slope and Adaptive Thresholding for Real-time ECG Signal Analysis

Masoomeh Rahimpour
R&D Department
Pooyandegan Rah Saadat Co.
Tehran, Iran
m.rahimpour@saadatco.com

Masoud Elhami Asl
R&D Department
Pooyandegan Rah Saadat Co.
Tehran, Iran
m.elhamiasl@saadatco.com

Mahmoud Reza Merati
R&D Department
Pooyandegan Rah Saadat Co.
Tehran, Iran
m.merati@saadatco.com

***Abstract*—The proper performance of a computerized ECG analysis is highly dependent on the accuracy of the extracted fiducial points. The aim of this paper is to develop an ECG analysis algorithm which analyzes all 12 lead ECG signals simultaneously and determines global durations and intervals including P duration, PQ interval, QRS duration, and QT interval. The basic concepts of this algorithm is based on the method previously introduced for automatic detection of wave boundaries based on the slope and adaptive thresholding. The method of identification of QRS complex type, QRS classification, and threshold determination were significantly modified considering the morphological features of each signal. These modifications led to less computational complexity for implementing on Electrocardiography system and high accuracy to be adaptable with medical standard requirements. On the other hand a novel algorithm for calculating the heart axis have been presented; performing based on combination of limb leads, this algorithm greatly reduces error rate in heart axis determination. For performance evaluation, both ECG data collected in Rajaie cardiovascular center and the CSE database are used. Mean difference and standard deviation of measurement results in millisecond unit estimated by proposed method vs CSE reference values are 0.7 and 3.70 for P duration, 1.40 and 3.52 for PQ interval, -1.10 and 3.04 for QRS duration, and 4.09 and 5.61 for QT interval.**

I. Introduction

ECG signal is one of the major physiological signals generated from heart's rhythmic polarization and depolarization. This signal is characterized by a number of waves as P, QRS, and T related to the heart activity. These parameters are useful characters for physicians in the heart disease diagnostic process. Modern digital electrocardiographs are capable of simultaneous 12-lead signal acquisition providing computer-based analysis of ECG waveforms which have reported global duration and intervals such as P and QRS durations, PR and PQ intervals, and heart axis [1].

Different methods for ECG wave's boundaries detection have been proposed in the literature, such as differentiated low-pass filtering [2], mathematical transforms [3], adaptive filters [4], classification methods (neural network, fuzzy algorithm) [5], and a combination of hidden Markov model and wavelet [6].

In this study, our aim is developing an ECG analysis algorithm which performs based on simultaneous 12 lead ECG signal and determines the global duration, intervals, and axis with high precision. We use similar idea presented in [2] for automatic detection of wave boundaries which is based on the slope feature and adaptive thresholding. The way of identifying the type of QRS complex, QRS classification, and determining the thresholds significantly modified by considering the morphological features of each signal. These modifications led to less computational complexity for implementing on Electrocardiograph device and high precision to meet medical standard requirements. On the other hand a novel algorithm for calculating the heart axis have been proposed. Performing based on combination of four limb leads signal (I, II, III and aVF), this algorithm greatly reduces error rate in heart axis determination.

II. Proposed Method

Measurement algorithm is based on analyzing 10-second 12 leads ECG signal. To remove different artifacts and improve the quality of signal, a 50 or 60 Hz notch filter to eliminate any AC interface and a linear second order band-pass filter, known as Lynn filter [7] with the frequency band of 0.8-18 Hz, have been applied to the input signal. The next step of measurement algorithm is R wave detection, which is necessary to beat segmentation. In this paper, R wave detection was accomplished based on well-known Pan-Tompkins algorithm [8] and applied on the signal of lead II; then the accurate location of R peaks on other leads was determined based on windowing technique around the approximated point called PK_i.

A. QRS complex boundary detection

According to the peak point detected as a R wave, each beat has been segmented and analyzed to estimate the onset and offset points of QRS complex and its amplitude. Extracting main features of QRS complex including QRS duration, R−R interval and R wave peak to peak amplitude is the next step; it identifies the class to which each complex belongs.

The positive and negative slopes before and after PK_i provide basic information about the onset and offset points of QRS complex. The nearest local extremum points in the original signal before and after the upward and downward going sides of the PK_i peak have been detected. The first points backward and forward these peaks in the differentiated

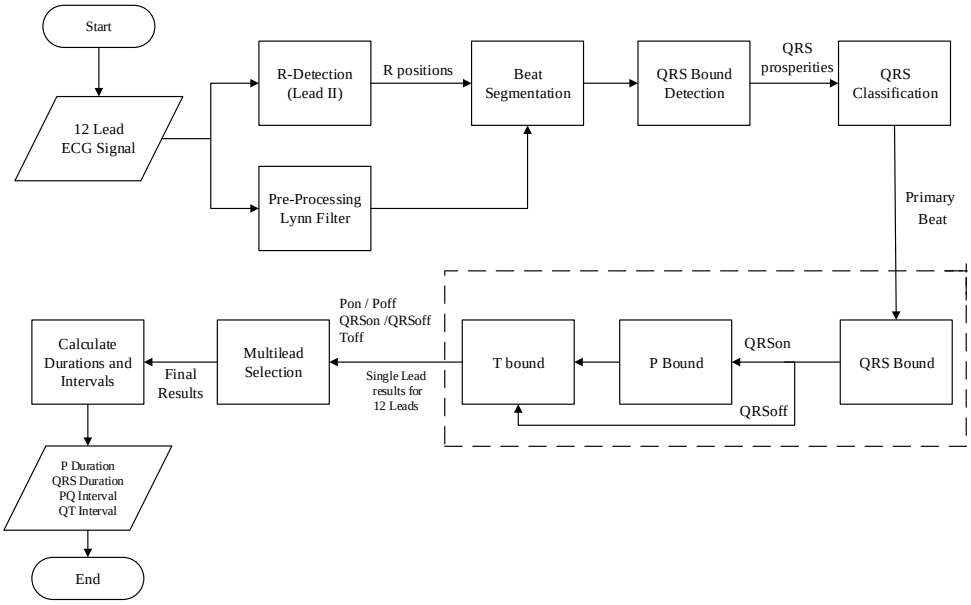

Fig. 1. General block diagram of measurement algorithm.

signal crossing the determined threshold and having slope values with opposite signs compared with the positive and negative slopes around PK_i, are approximated points for QRS complex onset and offset, respectively. Thresholds used in this step, are determined based on maximum and minimum slope values around the PK_i and some constant values according to presence of each wave (Q or S wave). In rest of the paper, $Imax$ and $Imin$ represent the maximum and minimum slope values.

B. QRS classification and type definition

In this stage a feature-based decision rule gives the beat to be processed. This classification logic has to allow for a single normally conducted beat. It decides based on the following features: QRS complex peak to peak amplitude, QRS duration and RR interval to exclude the extrasystoles. The aim is to choose one beat of a similar morphology as being conducted in the normal sequence through the ventricular. The classification method used here, is similar to the method used in Kenz electrocardiograph system [9]. Three classes are considered in order to beat classification including ”0” type as a normal beat, ”1” type as a normal beat with the shorten R−R interval which has laid before the abnormal beat, and ”2” type as an abnormal ECG beat. After beat classification, only one beat would be selected as the primary beat to be analyzed according to dominant method as mentioned in the following. In presence of abnormal beats, ECG beat with longest R-R interval extracted from ”0” type of QRS complexes, must be chosen as the primary beat. If type ”2” of QRS complex is present, ECG beats before and after the ”2” type QRS complexes are exempted from the object ECG wave. If ”0” type of QRS complex is absent, ECG beat of type ”1” with longest R−R interval must be extracted as the primary beat to avoid PVCs to be selected as a primary beat. In presence of normal rhythm, if all QRS complexes are considered as ”0” type, the 3rd beat must be chosen as the primary beat.

Generally 6 different types have been considered for QRS complex. These are including RSR’, QR, QRS, RS, R and QS types which was shown in Figure 2. Given these various types had a significant influence on accuracy of final detection results. Identifying the type of QRS complex is done according to the initial estimation of peak points on this complex known as PK_i; these points are the candidates of Q, R, S and R’ waves according to their amplitude and upward or downward slopes. There are two general morphology classes according to the sign of PK_i: In each class, the nearest local maximum before and after PK_i must be investigated to detect the other waves including Q, S and R’. In the algorithm 1, the method of type identification for RSR’ and rSr’ morphologies are explained as an instance.

According to the Figure 3, if the above conditions are correct just for the $previous\ max$, then the complex type would be RS; if they are correct just for the $next\ max$, the complex type would be QR and if they are correct for both of these points, it would imply the presence of rSr’ complex; eventually if these conditions are not applicable for none of these points, it would imply the presence of QS complex. Based on mentioned conditions, the accurate location of R, S and R’ or r, S and r’ have been detected and used to find the onset and offset points of QRS complex.

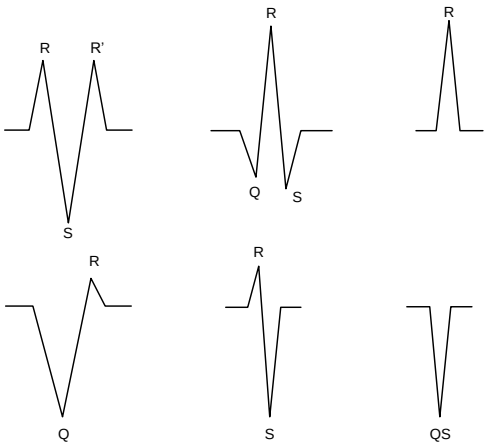

Fig. 2. Different types of QRS Complex (RSR', QR, R, QRS, RS, and QS).

Algorithm 1 RSR' and rSr' type identification

Input: QRS complex and PK_i
Output: accurate position of Q, R, and S wave.

```
Find the nearest local maximum before and after PK_i
if PK_i > 0 (according to Figure 3(a)) then
    if T_1 < 80 ms then
        if A_1 > A_2/4 then
            if Slope in point 2 > 1/15 Slope in point 1 then
                if Amplitude in point 3 < 0 then
                    return RSR' type
                end if
            end if
        end if
    end if
else
    if PK_i < 0 (according to Figure 3(b)) then
        if Amplitud of local maximum > Baseline then
            if Slope in point 2 > 1/15 Slope in point 1 then
                if Slope in point 4 > 1/15 Slope in point 3 then
                    if T1 < 75 ms and T2 < 75 ms then
                        return rSr' type
                    end if
                end if
            end if
        end if
    end if
end if
```

C. Wave boundary detection

After type declaration of QRS complex, the onset and offset points of each wave has determined within the windows locating according to the R wave. The method of boundary detection for each wave is described in the following.

1) QRS complex: A window with the width of 40 ms starting from $Imax$, backwards to P wave, has been located; based on the minimum and maximum value within this interval, the presence or absence of Q wave has been determined; the threshold value, TH_q, has defined by dividing the value of differentiated signal in this point to a constant value; if there is a Q wave, the constant of K_q and otherwise, the constant

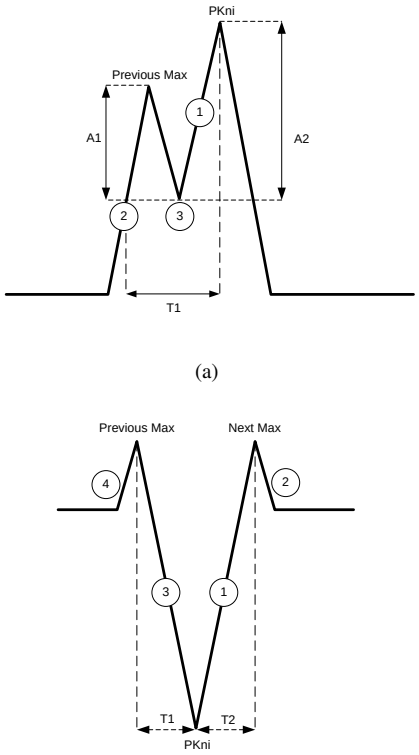

Fig. 3. QRS complex morphology in presence of (a) RSR' and (b) rSr'.

of K_r has been used to threshold selection for QRS onset determination.

This process has been done for QRS offset determination using a window with the width of 60 ms starting from $Imin$ towards T wave; constant value used in threshold selection takes the value K_s, if S wave is present and K_r if S wave is not present.

2) P wave: P wave analysis has been done within the interval preceding the QRS complex. Considering the onset of QRS complex, a window starting from 260 ms and ending at 30 ms before the Q wave has been used. The minimum and maximum values on the derivative signal are searched in this window; according to the amplitude of these points, the length of this window would be changed; this moving window has decreased the number of P waves falsely detected in the case of large PR intervals. The baseline level of signal is calculated based on average value of signal within the limit of P wave offset and QRS onset and P wave amplitude is determined relative to this level.

Considering P wave morphology, the threshold value for determination the fiducial limits of P wave, is calculated; for the positive slope located before (after) the negative slope, we consider upward-downward (downward-upward) shape for P wave; in each case the minimum and maximum slopes dividing to a constant values have been determined the threshold value. The offset point of P wave, P_2, has been defined as a backward point from the QRS onset where the processed signal reaches to the threshold $TH_{pe} = f(i_{max})/K_{pe}$ and the

onset point, P_1, has been defined as a backward point from P_2 where the processed signal reaches to the threshold $TH_{pb} = f(i_{min})/K_{pb}$. K_{pb} and K_{pe} are experimental and have their best performance for 1.35 and 2 respectively. According to the P wave morphology, the minimum or maximum point has been detected within the limit of P_1 and P_2 and marked as a P wave Peak P_p; to decrease the false positive errors caused by noise, the amplitude and duration of P wave is compared with acceptable limits (amplitude of P wave is measured related to the signal's noise level); if these parameters are in normal range, there is a definite P wave with determined fiducial points, otherwise there is no P wave in selected beat.

3) T wave: T wave boundaries have searched in a window starting from 50 ms and ending at $0.6\sqrt{R-R}$ after the R wave. This is an adaptive windowing which its length has modified according to the slope of signal at the ending 30% of window; in this part of window having a couple of maximum and minimum point on the derivative signal with comparable slope to their corresponding values in the beginning 70% of this window, indicates that P wave is located very close to T wave; therefore, the length of search window must be decreased. Shrinking the length of window occurred in gradual steps to decrease the probability of error and it would be more advantageous to avoid the next P wave being detected as a false T wave.

In this study the minimum length of this window is considered as $0.4(R-R)$, which is based on the borderline value for QT_c ($QT_c \geq 440ms$) [10] and Bazett's formula ($QT_c = QT/\sqrt{R-R}$).

In order to compare the maximum points located at the ending 30% of window with corresponding values in the beginning 70% of this window, K_{tp} constant value equal to 1.75 has been used. The method of finding onset and offset points of T wave is similar to what is used about P wave; this is according to thresholds defining based on minimum and maximum slope values in the specified window. The peak point of T wave is also determined by finding the zero crossing point in the derivative signal located within the limit of T wave onset and offset.

D. Multi Lead selection algorithm

Physiologically, the global durations of P, QRS and T waves are defined by the earliest onset in one lead and the latest offset in any other lead; indeed wave onset and offset do not necessarily appear at the same time in all leads, because the activation propagate differently [11]. Considering this issue, we used a Multi-lead algorithm to select the final value of parameters; this method will reduce the influence of possible noisy measurements. The post-processing rules for fiducial point detection consist of ordering the preliminary results and selecting the onset (offset) point of each wave as first (last) points which k nearest neighbors lay within an $(\delta)ms$ interval. The value of δ has selected empirically and is based on usual variability in manual annotations [12]. This is considered as $\delta = 6ms$ for P and QRS onset and P offset, $\delta = 10ms$ for QRS offset and $\delta = 12ms$ for T offset [13]. Applying this method, a single missing lead would not necessarily cause of rejecting the whole 12 ECG lead.

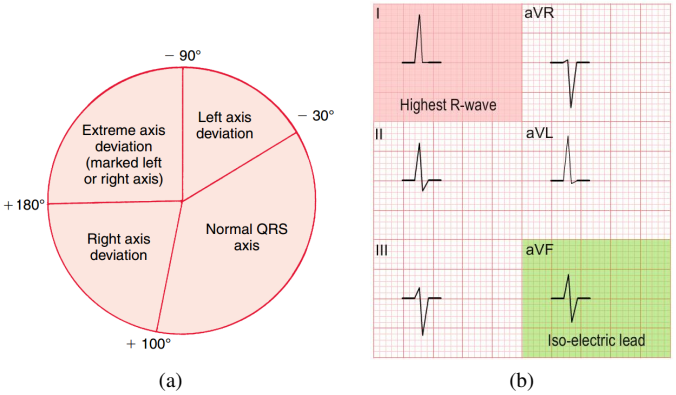

(a) (b)

Fig. 4. (a) Normal and abnormal limits for QRS axis [18], (b) An example of iso-electric method for heart axis calculation.

E. Heart axis calculation

Heart axis calculation are one of the most important part of the computerized electrocardiography system. In clinical applications, these parameters provide helpful information for medical diagnosis [14]. Figure 4(a) shows the normal and abnormal limits for QRS axis. The electrical axis of the heart is the mean direction of action potentials traveling through the ventricles during ventricular activation (depolarization). The QRS complex which represents ventricular depolarization is more common to determine the frontal electrical heart axis.

Any combination of 2 limb leads can be used to calculate the QRS frontal axis[15]. Some of well-known equations to calculate QRS axis are introduced in Table I [16], [17]. In this equations "I" is net voltage of QRS wave in lead I and so on. Using lead having maximum net amplitude, leads to more accurate result.

A common method among physicians for heart axis determination is iso-electric method. Iso-electric lead contains biphasic waves with approximately zero net amplitude which the QRS axis is perpendicular to its orientation Figure 4(b). In proposed method, we have used optimized combination of 2 leads with highest amplitudes to achieve more accurate result. By choosing 2 leads with maximum net amplitudes, the QRS axis would be calculated according to the equations defined in Table I.

TABLE I. DEFINED EQUATIONS FOR HEART AXIS CALCULATION BASED ON SELECTED LEADS.

Selected Leads	Equation
I and aVF	$\alpha = \tan^{-1}(2aVF/\sqrt{3}I)$
I and II	$\alpha = \tan^{-1}((2II - I)/\sqrt{3}I)$
I and III	$\alpha = \tan^{-1}((I + 2III)/\sqrt{3}I)$
II and III	$\alpha = \tan^{-1}((II + III)/\sqrt{3}(II - III))$

III. RESULTS

The proposed method has been implemented in Visual Studio C++ 2010. We consider two databases for performance evaluation of this method, CSE Multi-lead database and ECG data collected in Rajaie cardiovascular, medical and research

center (RCMRC); CSE (Common Standard for Quantitative Electrocardiography) is a reference database are being used by more than 110 academic and industry research centers in order to assess and improve ECG measurement and interpretation programs. The quality assurance rules promoted by CTS-ECG are now part of IEC 60601-2-25 standard [11]. This database contains 125 records each of them lasting 10 seconds with the sampling frequency of 500 Hz [19].

Using the proposed method, the duration, intervals and heart axis of ECG signals have been calculated for both CSE database and collected dataset. Deviation of these measurements from the mean referee estimates of CSE database and RCMRC physician's annotations are presented in Table II and III; the acceptable limits for these parameters recommended in Table 201.105 of IEC-60601-2-25 standard [11] are mentioned in these tables. For detailed analysis of the results, the boxplot of these deviations for all records are shown in Figure 5. According to these plots, the concentration of measurement errors have laid in the acceptable limits mentioned in standard. In addition, they indicate that the proposed algorithm has the uniform performance in measuring different parameters. Figure 6, also shows the typical results of the algorithms for different ECG signals.

In order to investigate the validity of measurement results, we have compared the proposed algorithm to the ecgpuwave algorithm which is a well-known approach of fiducial points extraction. The results of this comparison are provided in Table II which show a significant improvement in ECG wave boundaries detection using the proposed method. Using adaptive windowing and considering the morphology of each wave, lead to more enhanced results in comparison to ecgpuwave approach.

Another point of interest is to investigate the performance of proposed algorithm in presence of noisy signals specially EMG noise. The results shows that the algorithm is largely robust against the noise; on the other hand, we previously developed a dynamic Gaussian filter [20] which suppresses the noise significantly and enhances the results of wave boundaries detection. Table IV shows the improvement of detection results after applying EMG filter as a preprocessing step on the input signals especially in the case of P and T wave duration.

Table V depicts the mean and standard deviation of the difference between calculated axis by proposed method and physician annotations for P, QRS, and T axis. Comparing the results of heart axis calculation to physician's annotations indicates the acceptable performance of proposed algorithm.

IV. Conclusion

In this paper, we proposed an efficient algorithm to automatic measurement of duration, intervals and axis in 12 lead ECG signal. Using the adaptive thresholds and moving windows according to the morphologic features of the signal have profoundly improved the performance of proposed algorithm. Additionally, using the slope feature to extract the fiducial points, make this method less complex and simple to implement which is required for real-time industrial applications. In the future study, we are going to use these measurement results for automatic ECG signal interpretation.

Although the proposed algorithm has a great potential in measuring the major parameters for variety of ECG morphologies, the presence of unpredictable morphologies in clinical conditions may lead to partially unreliable results; therefore, for diagnostic applications there is a need for evaluation with more clinically recorded signals.

TABLE II. The result of ECGpuwave vs proposed method on CSE database.

	Mean Difference (ms)			**Standard Deviation**		
	Standard	ECG-puwave	Proposed method	Standard	ECG-puwave	Proposed method
P Duration	±10	7.35	0.70	15	10.27	3.70
QRS Duration	±10	7.77	1.40	10	14.51	3.52
PQ Interval	±10	2.5	-1.1	10	10.73	3.04
QT Interval	±25	-7.57	4.09	30	35.29	5.61

TABLE III. Mean difference and standard deviation for global duration and intervals on collected dataset in RCMRC.

	Mean Difference (ms)		**Standard Deviation**	
	Standard	Proposed method	Standard	Proposed method
P Duration	±10	2.23	15	4.65
QRS Duration	±10	3.08	10	4.23
PQ Interval	±10	1.48	10	4.42
QT Interval	±25	7.19	30	8.79

TABLE IV. Mean difference and standard deviation for global duration and intervals on CSE database with and without applying EMG filter.

	Mean Difference (ms)			**Standard Deviation**		
	Standard	Proposed method	Apply EMG Filter	Standard	Proposed method	Apply EMG Filter
P Duration	±10	0.70	0.61	15	3.70	3.56
QRS Duration	±10	1.40	1.43	10	3.52	2.89
PQ Interval	±10	-1.10	-0.94	10	3.04	2.78
QT Interval	±25	4.09	3.94	30	5.61	5.23

TABLE V. Mean difference and standard deviation for P, QRS, and T axis on CSE database and collected dataset in RCMRC

	Mean Difference (in degree)			**Standard Deviation**		
	P axis	QRS axis	T axis	axis	QRS axis	T axis
CSE DB	2.99	0.59	1.05	21.54	15.44	19.18
RCMRC DB	3.54	2.65	-2.86	23.15	17.63	16.53

References

[1] P. Kligfield, F. Badilini, I. Rowlandson *et al.*, "Comparison of automated measurements of electrocardiographic intervals and durations by computer-based algorithms of digital electrocardiographs," *The American Heart journal*, vol. 167, no. 2, pp. 150–159, 2014.

[2] P. Laguna, R. Jané, and P. Caminal, "Automatic detection of wave boundaries in multilead ecg signals: validation with the cse database," *Computers and biomedical research*, vol. 27, no. 1, pp. 45–60, 1994.

[3] J. P. Martínez, R. Almeida, S. Olmos, A. P. Rocha, and P. Laguna, "A wavelet-based ecg delineator: evaluation on standard databases," *Biomedical Engineering, IEEE Transactions on*, vol. 51, no. 4, pp. 570–581, 2004.

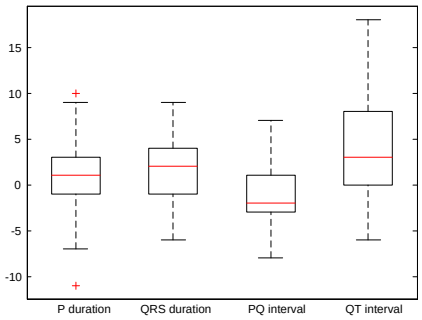

(a)

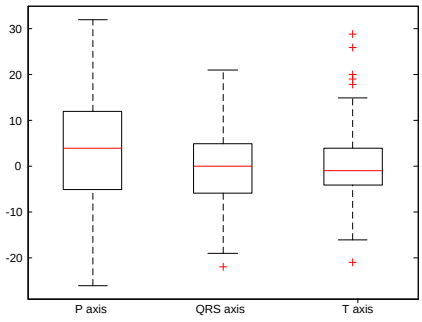

(b)

Fig. 5. Boxplot of deviations between measurements obtained by proposed method and reference values for (a) P duration, QRS duration, PQ interval and QT interval and (b) heart axis for P, QRS, and T waves.

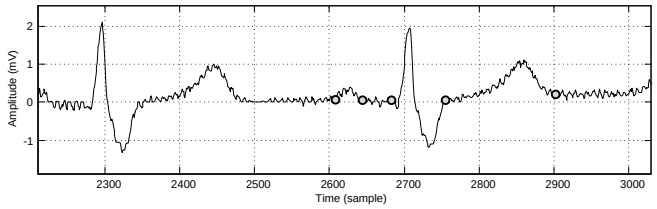

(a)

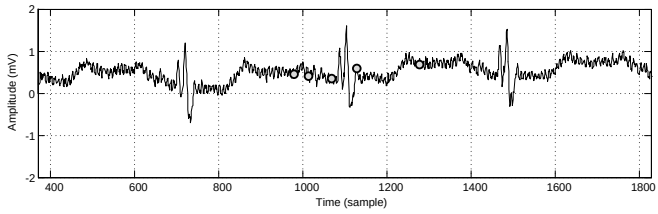

(b)

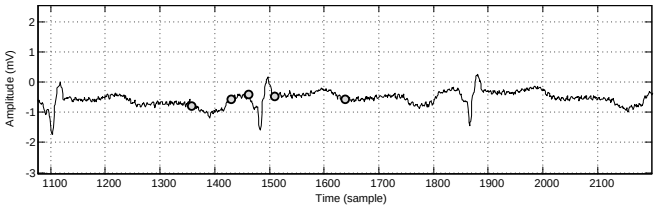

(c)

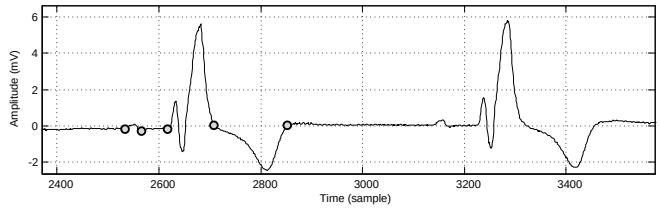

(d)

Fig. 6. Typical results of proposed algorithms for different ECG signals.

[4] A. Goutas, Y. Ferdi, J.-P. Herbeuval, M. Boudraa, and B. Boucheham, "Digital fractional order differentiation-based algorithm for p and t-waves detection and delineation," *ITBM-RBM*, vol. 26, no. 2, pp. 127–132, 2005.

[5] K. Sternickel, "Automatic pattern recognition in ecg time series," *Computer methods and programs in biomedicine*, vol. 68, no. 2, pp. 109–115, 2002.

[6] S. Graja and J.-M. Boucher, "Hidden markov tree model applied to ecg delineation," *Instrumentation and Measurement, IEEE Transactions on*, vol. 54, no. 6, pp. 2163–2168, 2005.

[7] P. Lynn, "Online digital filters for biological signals: some fast designs for a small computer," *Medical and Biological Engineering and Computing*, vol. 15, no. 5, pp. 534–540, 1977.

[8] J. Pan and W. J. Tompkins, "A real-time qrs detection algorithm," *Biomedical Engineering, IEEE Transactions on*, no. 3, pp. 230–236, 1985.

[9] SUZUKEN, "Kenz cardico: Physician criteria guide," 2009.

[10] J. N. Johnson and M. J. Ackerman, "Qtc: how long is too long?" *British journal of sports medicine*, vol. 43, no. 9, pp. 657–662, 2009.

[11] "International standard, IEC. 60601-2-51: Particular requirements for safety, including essential performance of recording and analysing single channel and multichannel electrocardiographs," *Edition 2.0*, 2011.

[12] P. Laguna, N. Thakor, P. Caminal, R. Jane, H.-R. Yoon, A. Bayes de Luna, V. Marti, and J. Guindo, "New algorithm for qt interval analysis in 24-hour holter ecg: performance and applications," *Medical and Biological Engineering and Computing*, vol. 28, no. 1, pp. 67–73, 1990.

[13] R. Almeida, J. P. Martinez, A. P. Rocha, and P. Laguna, "Multilead ecg delineation using spatially projected leads from wavelet transform loops," *Biomedical Engineering, IEEE Transactions on*, vol. 56, no. 8, pp. 1996–2005, 2009.

[14] D. H. Spodick, M. Frisella, and S. Apiyassawat, "Qrs axis validation in clinical electrocardiography," *The American journal of cardiology*, vol. 101, no. 2, pp. 268–269, 2008.

[15] S. Hoseini, A. Moeeny, S. Shoar, N. Shoar, M. Naderan, S. Gharibzadeh, and A. Dehpour, "Designing nomogram for determining the hearts qrs axis," *Journal of Clinical and Basic Cardiology*, vol. 14, no. 1, pp. 12–15, 2012.

[16] P. Singh and M. S. Athar, "Simplified calculation of mean qrs vector (mean electrical axis of heart) of electrocardiogram," *Indian journal of physiology and pharmacology*, vol. 47, no. 2, pp. 212–216, 2003.

[17] D. Novosel, G. Noll, and T. F. Lüscher, "Corrected formula for the calculation of the electrical heart axis," *Croatian medical journal*, vol. 40, pp. 77–79, 1999.

[18] A. L. Goldberger, *Clinical electrocardiography: a simplified approach*. Elsevier Health Sciences, 2012.

[19] J. Willems, P. Arnaud, J. Van Bemmel, R. Degani, P. Macfarlane, and C. Zywietz, "Common standards for quantitative electrocardiography: goals and main results. cse working party." *Methods of Information in Medicine*, vol. 29, no. 4, pp. 263–271, 1990.

[20] A. Hashemi, M. Rahimpour, and M. R. Merati, "Dynamic gaussian filter for muscle noise reduction in ecg signal," in *Electrical Engineering (ICEE), 2015 23rd Iranian Conference on*. IEEE, 2015, pp. 120–124.